

See discussions, stats, and author profiles for this publication at: <https://www.researchgate.net/publication/220023738>

Solvent-Induced Synthesis of Zinc(II) and Manganese(II) Coordination Polymers with a Semirigid Tetracarboxylic Acid

ARTICLE *in* CRYSTAL GROWTH & DESIGN · JUNE 2011

Impact Factor: 4.89 · DOI: 10.1021/Cg200229h

CITATIONS

41

READS

82

5 AUTHORS, INCLUDING:



Youlong Zhu

University of Colorado Boulder

11 PUBLICATIONS 246 CITATIONS

SEE PROFILE

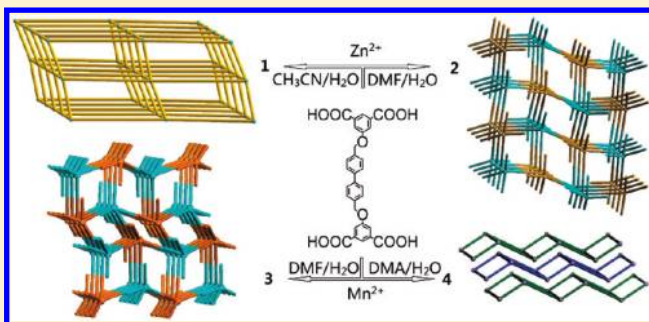
Solvent-Induced Synthesis of Zinc(II) and Manganese(II) Coordination Polymers with a Semirigid Tetracarboxylic Acid

Ling-Ling Qu, You-Long Zhu, Yi-Zhi Li, Hong-Bin Du,* and Xiao-Zeng You

State Key Laboratory of Coordination Chemistry, Nanjing National Laboratory of Microstructures, School of Chemistry, Chemical Engineering, Nanjing University, Nanjing, 210093, China

Supporting Information

ABSTRACT: By using a semirigid quadricarboxylate ligand 5,5'-(biphenyl-4,4'-diylbis(methylene))bis(oxy)diisophthalic acid (H_4L), four novel coordination polymers were obtained solvothermally and characterized by single-crystal X-ray diffraction, thermogravimetric, photoluminescent and gas adsorption studies. Compound $[Zn_2(L)] \cdot CH_3CN$, **1**, is a three-dimensional (3D) framework built from one-dimensional (1D) rod-shaped $Zn-O-C$ secondary building units (SBUs) that are linked together by the 4-connecting L ligands to give rod packing of **pcu** type and elliptical channels of $7.7 \times 8.4 \text{ \AA}^2$. Compound $[Zn_4(L)_2(H_2O)_4] \cdot 5H_2O$, **2**, possesses a 3D open framework with a doubly interpenetrated **sra** net built from 4-connecting $Zn_2(OOC)_4$ unit and L ligand. Compound $[Mn_2(L)(H_2O)_2] \cdot 2H_2O$, **3**, is built from trigonal–bipyramidal binuclear $Mn_2(OOC)_3$ units and octadentate L ligands, forming a binodal 5,5-connected $4^3.6^6.8$ net. Compound $[Mn(H_2L)(DMA)(H_2O)] \cdot (DMA)(H_2O)$, **4**, is a two-dimensional (2D) layered structure made of 4-connecting mononuclear Mn atoms and half-deprotonated L ligands. N_2 gas adsorption measurements at 77 K showed that compounds **1**, **2**, and **4** possess permanent porosities.



INTRODUCTION

The design and synthesis of multidimensional metal–organic frameworks (MOFs) have received remarkable attention not only due to their intriguing variety of structures but also to their potential applications in many fields such as luminescence, sorption, magnetism, and catalysis.¹ To date, however, how to rationally design and synthesize MOFs with the desired structure and properties is still a challenge because the formation of MOFs may be easily affected by many factors, such as organic ligands, metal ions, metal-to-ligand ratios, solvents, reaction temperature, and counterions.² Among these factors, organic ligands and metal ions play crucial roles in synthesizing new MOFs. Remarkable progress has been made in recent years in preparing MOFs by using multidentate aromatic carboxylic acid ligands as bridges or building blocks with metal ions or clusters as nodes.³ For example, various tetracarboxylate ligands (Scheme 1), such as 2,3,2',3'-oxidiphthalic acid (**L1**),⁴ biphenyl-3,4,3',4'-tetracarboxylic acid (**L2**),⁵ biphenyl-2,3,2',3'-tetracarboxylic acid (**L3**),⁶ 2,3,2',3'-thiodiphthalic acid (**L4**),⁷ (E)-5,5'-(diazene-1,2-diyl)diisophthalic acid (**L5**),⁸ 3,3',5,5'-biphenyltetracarboxylic acid (**L6**),^{9,10} quaterphenyl-3,3'',5,5'''-tetracarboxylic acid (**L7**),^{10,11} 5,5'-(propane-1,3-diylbis(oxy))diisophthalic acid (**L8**),¹² and 5,5'-(1,4-phenylenebis(methylene))bis(oxy)diisophthalic acid (**L9**)¹³ have been used to produce metal–organic coordination frameworks, due to their versatile bridge modes, and excellent coordination capacities.

We have been interested in preparing MOFs by using semirigid tetradentate ligands, for example, tetrakis(4-pyridyloxymethylene) methane¹⁴ and tetrakis[4-(carboxyphenyl)oxamethyl]methane acid.¹⁵ These tetrahedral ligands, from both zeolite chemistry and crystal engineering points of view, may result in highly porous frameworks with a low framework density. In addition, they are semirigid ligands, in which the four coordination centers can flexibly twist around to meet different coordination environments. Therefore, a number of MOFs built from these ligands have been reported,^{14–16} which exhibit rich structural topology. Following this strategy, we designed a new semirigid tetradentate ligand 5,5'-(biphenyl-4,4'-diylbis(methylene))bis(oxy)diisophthalic acid (H_4L) and synthesized four new coordination polymers of Zn and Mn by using this ligand under different solvent systems. Herein, we report their structural diversification and related properties such as thermal stability, fluorescence, and gas adsorption.

EXPERIMENTAL SECTION

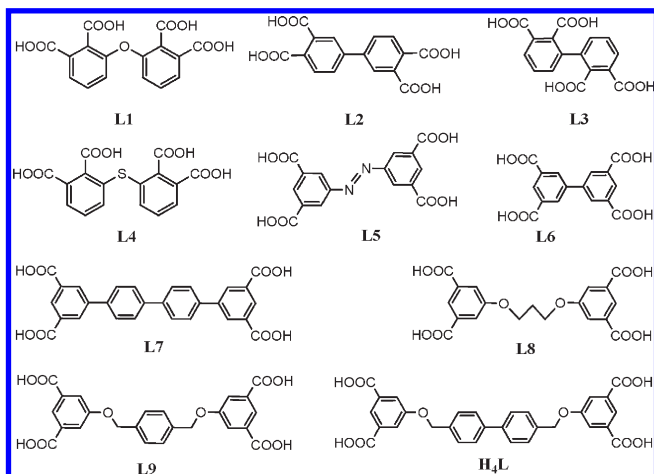
Materials and Methods. All reagents and solvents were purchased from commercial sources and used without further purification. Elemental analyses of C, H, and N were performed on a Perkin-Elmer

Received: February 19, 2011

Revised: April 25, 2011

Published: May 02, 2011

Scheme 1. Structures of Selected Tetracarboxylate Ligands



240C elemental analyzer. X-ray powder diffraction (XRPD) measurements were performed on a Bruker D8 diffractometer operated at 40 kV and 40 mA using a Cu K α radiation ($\lambda = 1.54056 \text{ \AA}$). Thermogravimetric analyses (TGA) were performed on a Perkin-Elmer thermal analyzer under nitrogen with a heating rate of $10 \text{ }^\circ\text{C/min}$. The N_2 adsorption isotherms were measured at 77 K by using a Micromeritics ASAP 2020M volumetric adsorption analyzer. The samples were pretreated at 373 K under a $50 \text{ }\mu\text{m Hg}$ vacuum for about 10 h prior to the measurement of the isotherms. Photoluminescence analyses were performed on a Hitachi 850 fluorescence spectrophotometer.

Synthesis of H_4L . The H_4L ligand was synthesized by a two-step procedure.¹⁷ First, a mixture of 10.0 mmol of dimethyl-5-hydroxyisophthalate, 4.90 mmol of 4,4'-bis(chloromethyl)biphenyl, 16.0 mmol of K_2CO_3 , 0.10 g of 18-crown-6 ether, and 40 mL of THF was stirred under N_2 at $65 \text{ }^\circ\text{C}$ for 48 h. The mixture was concentrated, and 20 mL of 1% aqueous Na_2CO_3 was added at $0 \text{ }^\circ\text{C}$. A white solid (E1) was obtained by filter, washed with water, and dried under a vacuum at $50 \text{ }^\circ\text{C}$. Yield 80%. Second, 2.0 mmol of E1 and 8.1 mmol of KOH were dissolved in 30 mL of methanol/water (1:1 in volume). The reaction mixture was refluxed for 48 h at $65 \text{ }^\circ\text{C}$. The mixture was concentrated, and acidified with 6 M aqueous HCl at $0 \text{ }^\circ\text{C}$. The precipitate was collected, washed with water, and dried under a vacuum at $50 \text{ }^\circ\text{C}$. Yield: 60%. $^1\text{H NMR}$ ($\text{DMSO}-d_6$): 5.304 (4H, s), 7.578 (4H, d), 7.736 (4H, d), 7.765 (4H, s), 8.098 (2H, s), 13.313 (4H, s).

Synthesis of $[\text{Zn}_2(\text{L})] \cdot \text{CH}_3\text{CN}$ (1). A mixture of H_4L (10.8 mg, 0.02 mmol), $\text{Zn}(\text{NO}_3)_2 \cdot 6\text{H}_2\text{O}$ (11.9 mg, 0.04 mmol), water (2 mL), acetonitrile (4 mL), and 3 drops of 2 M HAc was sealed in the autoclave at $120 \text{ }^\circ\text{C}$ for 3 days. Yellow block crystals of 1 were obtained by filtration and washed by water and ethanol several times with a yield of 86% (based on Zn salts). Anal. Calcd for $\text{C}_{32}\text{H}_{21}\text{NO}_{10}\text{Zn}_2$ (%): C, 54.07; H, 2.96; N, 1.97. Found: C, 54.10; H, 3.00; N, 1.52.

Synthesis of $[\text{Zn}_4(\text{L})_2(\text{H}_2\text{O})_4] \cdot 5\text{H}_2\text{O}$ (2). The preparation of 2 was similar to that of 1 except that N,N -dimethylformamide (DMF) was used instead of acetonitrile. Colorless platelet crystals of 2 were collected (87% yield based on Zn salts). Anal. Calcd for $\text{C}_{60}\text{H}_{54}\text{O}_{29}\text{Zn}_4$ (%): C, 47.98; H, 3.60. Found: C, 48.01; H, 3.61.

Synthesis of $[\text{Mn}_2(\text{L})(\text{H}_2\text{O})_2] \cdot 2\text{H}_2\text{O}$ (3). Complex 3 was obtained by the same procedure used for preparation of 2 except that $\text{MnCl}_2 \cdot 4\text{H}_2\text{O}$ (7.9 mg, 0.04 mmol) was used instead of $\text{Zn}(\text{NO}_3)_2 \cdot 6\text{H}_2\text{O}$ as a starting material. Yellow block crystals of 3 were obtained by filtration and washed by water and ethanol for several times with a yield of 68% (based on Mn salts). Anal. Calcd for $\text{C}_{30}\text{H}_{26}\text{Mn}_2\text{O}_{14}$ (%): C, 49.97; H, 3.61. Found: C, 50.23; H, 3.98.

Synthesis of $[\text{Mn}(\text{H}_2\text{L})(\text{DMA})(\text{H}_2\text{O})] \cdot (\text{DMA})(\text{H}_2\text{O})$ (4). When N,N -dimethylacetamide (DMA) instead of DMF was used as solvent,

compound 4 was obtained by following the procedures used for preparation of 3. Colorless platelet crystals of 4 were collected by filtration and washed by water and ethanol several times with a yield of 50% (based on Mn salts). Anal. Calcd for $\text{C}_{38}\text{H}_{42}\text{MnN}_2\text{O}_{14}$ (%): C, 56.60; H, 5.21; N, 3.48. Found: C, 56.23; H, 5.54; N, 3.46.

Single-Crystal X-ray Diffraction Analysis. Suitable single crystals of complexes 1–4 were mounted on a Bruker Smart Apex CCD diffractometer with graphite-monochromated Mo K α radiation ($\lambda = 0.71073 \text{ \AA}$) at $20(2) \text{ }^\circ\text{C}$ using the ω -scan technique. Data reductions and absorption corrections were performed using the SAINT and SADABS programs,¹⁸ respectively. The structures were solved by direct methods and all non-hydrogen atoms were refined anisotropically on F^2 by the full-matrix least-squares technique using the SHELXL-97 crystallographic software package.¹⁹ All the hydrogen atoms were placed in geometrically calculated positions and refined using the riding model. The relevant crystallographic data are presented in Table 1. Selected bond lengths and angles for 1–4 are listed in Table S1 in the Supporting Information.

RESULTS AND DISCUSSION

Synthesis. Compounds 1–4 were obtained under similar solvothermal conditions by using quadricarboxylate ligand H_4L . The as-synthesized products are of pure phase as confirmed by XRPD analyses (Figure S1, Supporting Information). It is noted that the counteranions used in the metal salts had little effect on the final products. In other words, use of metal salts of nitrate, chloride, or acetate all led to the same products. However, the formations of 1–4 were shown to be strongly dependent on the solvent: The Zn complexes 1 and 2 were obtained from respective $\text{CH}_3\text{CN}-\text{H}_2\text{O}$ and $\text{DMF}-\text{H}_2\text{O}$ systems; the Mn complexes 3 and 4 were formed by using $\text{DMF}-\text{H}_2\text{O}$ and $\text{DMA}-\text{H}_2\text{O}$ solvents under the otherwise same conditions, respectively. X-ray crystal structure analyses revealed that only CH_3CN and DMA were incorporated into the final products of 1 and 4. Such profound effects of the solvent on the self-assembly process have been known,²⁰ which have been attributed to their respective size, shape, and coordination ability. Complexes 2 and 3, both prepared from the $\text{DMF}-\text{H}_2\text{O}$ solvent system, possess different structures, which may be likely due to the different coordination abilities of the metal ions.

Crystal Structures. **$[\text{Zn}_2(\text{L})] \cdot \text{CH}_3\text{CN}$ (1).** Compound 1 crystallizes in a monoclinic space group $\text{C2}/c$. The asymmetric unit of 1 consists of one Zn atom, half of a ligand L, and one acetonitrile guest molecule. As shown in Figure 1, the Zn atom is in a distorted tetrahedral geometry, coordinated by four O atoms from four different L ligands with the Zn–O distances ranging from 1.907(3) to 1.969(3) \AA . The bond angles around the Zn atom are in the range of $98.64(13)–123.49(13)^\circ$. The L ligand is fully deprotonated and connects to eight Zn atoms in bis-monodenate coordination fashion. It is in a nearly planar geometry with the center sitting on a 2-fold symmetry axis. The dihedral angles are $23.0(2)$ and $10.3(2)^\circ$ between the two middle biphenyl and two side-middle phenyl rings, respectively. The ligands are parallel aligned and interconnected with neighboring ones via common Zn atoms to form a 2D sheet with elliptical rings of $7.7 \times 21.1 \text{ \AA}^2$ in diameters (Figure 2). The 2D sheets stack in an eclipsed manner along the c -axis and interlink with each other via sharing common O vertices on the ZnO_4 tetrahedra between two adjacent layers. This gives rise to a 3D framework with one-dimensional elliptical ring channels along the c -axis. Inside the channels reside the disordered acetonitrile molecules as guests, which form weak van der Waals interactions

with the host framework. PLATON²¹ calculations show that the guest accessible volume (521.9 Å³ per unit cell) comprises 17.8% of the unit cell volume.

From a topological viewpoint, the framework of **1** can be viewed as constructed from rod-shaped secondary building units (SBUs).²² As shown in Figure 3, the Zn–O–C rods are composed of 4-coordinated Zn centers that are bound by four carboxyl groups from four ligands. The rods run along the *c* crystallographic direction and are linked together by the 4-connecting ligands to four other rods to give rod packing of *pcu* type and elliptical channels of 7.7×8.4 Å² in the *c* direction.

[Zn₄(L)₂(H₂O)₄]·5H₂O (**2**). Compound **2** crystallizes in the monoclinic space group *P*₂₁/*c*. The asymmetric unit consists of two Zn centers, one L ligand, two coordinate, and five guest water molecules. Of the two Zn atoms (Figure 4), Zn1 is five-coordinated by three carboxylate oxygen atoms from three L ligands and two water oxygen atoms, while Zn2 is in a distorted tetrahedral geometry, coordinated by four oxygen atoms from four L ligands. The two Zn atoms are linked together by four carboxyl groups to form a binuclear tetrahedral unit. The bond lengths of Zn–O are comparable to the other reported Zn(II) carboxyl complexes.^{14a,c,15c,23} Similar to that in **1**, the ligand L is fully deprotonated and adopts a nearly planar coordination geometry. However, the ligand L in **2** connects to only seven Zn atoms in monodenate coordination fashion with the eighth oxygen atom remaining uncoordinated. In addition, the four phenyl rings of L are not coplanar as in **1**. The two coplanar middle biphenyl rings of the L ligand in **2** are nearly perpendicular to the two side phenyl rings bearing the carboxyl groups. The dihedral angles are 3.7(1), 79.2(1)–86.4(1), and 11.4(1)° between the two middle biphenyl, the two side-middle, and the two side–side phenyl rings, respectively.

Compound **2** possesses a 3D framework built from 4-connecting Zn₂(OOC)₄ units and ligands L (Figure 5). The binuclear units are tetrahedrally linked by four carboxyl groups from four L ligands, while ligands L are connecting four Zn₂(OOC)₄ units. Considering the Zn₂(OOC)₄ unit and the L ligand as a respective 4-connecting node, the framework of **2** can thus be reduced to a known 4,4-connected *sra* net.²⁴ The net is 2-fold interpenetrated, which eliminates parts of its large voids. Small rectangular pore channels measuring 8.5×9.5 Å² run along the *a* axis, in which water molecules reside as guests. The guest water molecules form extensive hydrogen bonds with the framework atoms (Table S2, Supporting Information) to stabilize the structure. PLATON²¹ calculations show that the guest accessible volume (1084.4 Å³ per unit cell) comprises 29.9% of the unit cell volume.

[Mn₂(L)(H₂O)₂]·2H₂O (**3**). Compound **3** crystallizes in the monoclinic space group *P*₂₁/*c*. The asymmetric unit in **3** consists of two Mn(II) cations, one L ligand, two coordinate, and two

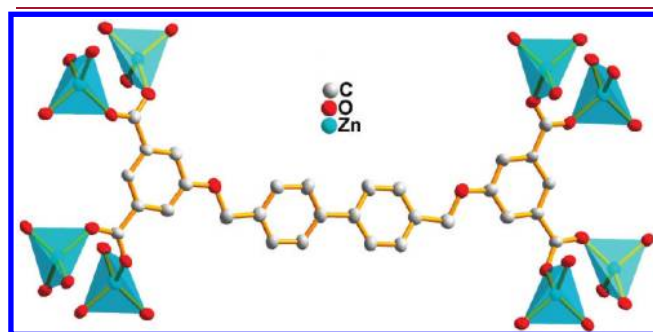


Figure 1. Building units of **1** (ellipsoids drawn at the 50% probability).

Table 1. Crystallographic and Structural Data for **1–4**

compound reference	1	2	3	4
chemical formula	C ₃₂ H ₂₁ NO ₁₀ Zn ₂	C ₆₀ H ₅₄ O ₂₉ Zn ₄	C ₃₀ H ₂₆ Mn ₂ O ₁₄	C ₃₈ H ₄₂ MnN ₂ O ₁₄
formula mass	710.24	1500.51	720.39	805.68
crystal system	monoclinic	monoclinic	monoclinic	triclinic
<i>a</i> /Å	23.482(3)	9.3243(9)	8.6801(11)	10.4542(8)
<i>b</i> /Å	16.7231(18)	26.939(3)	28.708(4)	13.8140(10)
<i>c</i> /Å	7.7066(8)	14.4535(14)	13.9279(18)	13.9456(11)
α /°	90.00	90.00	90.00	77.0740(10)
β /°	104.716(2)	93.0680(10)	90.910(2)	78.2320(10)
γ /°	90.00	90.00	90.00	76.9100(10)
unit cell volume/Å ³	2927.0(5)	3625.4(6)	3470.2(8)	1886.8(2)
temperature/K	291(2)	291(2)	291(2)	291(2)
space group	<i>C</i> 2/ <i>c</i>	<i>P</i> ₂ ₁ / <i>c</i>	<i>P</i> ₂ ₁ / <i>c</i>	<i>P</i> $\bar{1}$
no. of formula units per unit cell, <i>Z</i>	4	2	4	2
absorption coefficient, μ /mm ^{−1}	1.701	1.385	0.790	0.422
no. of reflections measured	7841	19776	18895	10409
no. of independent reflections	2874	7104	6806	7272
<i>R</i> _{int}	0.0386	0.0496	0.0315	0.0255
final <i>R</i> ₁ values (<i>I</i> > 2σ(<i>I</i>)) ^a	0.0563	0.0451	0.0491	0.0613
final <i>wR</i> (<i>F</i> ²) values (<i>I</i> > 2σ(<i>I</i>)) ^a	0.1421	0.0925	0.1327	0.1403
final <i>R</i> ₁ values (all data) ^a	0.0757	0.0762	0.0646	0.0802
final <i>wR</i> (<i>F</i> ²) values (all data) ^a	0.1483	0.0987	0.1380	0.1456
goodness of fit on <i>F</i> ²	1.096	1.013	1.077	1.081
CCDC number	810254	810255	810256	810257

^a $R_1 = \sum |F_o| - |F_c|$, $wR = [\sum w(F_o^2 - F_c^2)^2 / \sum w(F_o^2)^2]^{1/2}$.

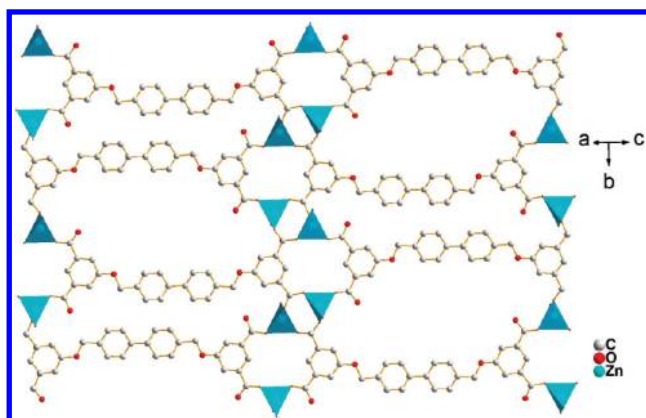


Figure 2. A single layer in **1** with Zn shown as polyhedra.

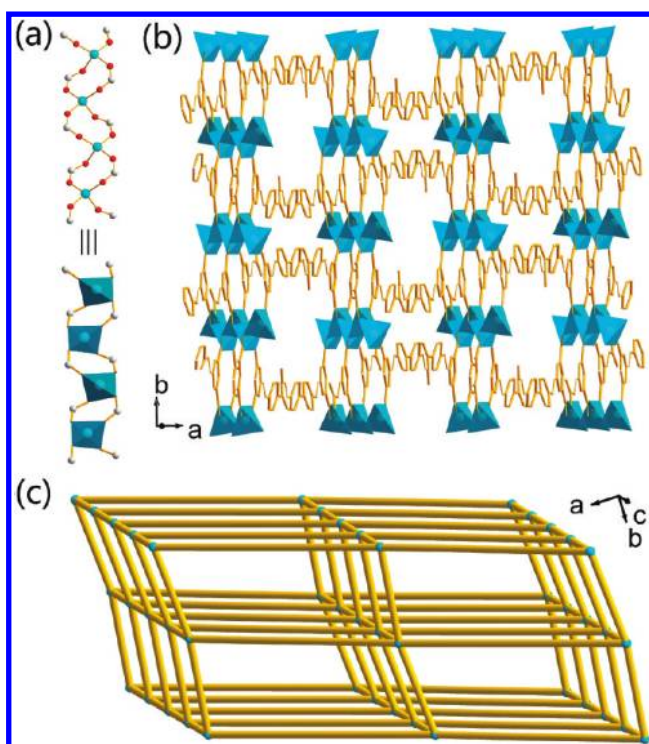


Figure 3. Views of (a) rod-shaped SBUs, (b) 3D framework with inorganic SBUs linked together via *L*, and (c) topological view of **1**.

uncoordinate water molecules. Both Mn(II) centers are 5-coordinated by four different *L* ligands and one water molecule (Figure 6). However, their coordination geometries are slightly different. The angular structural parameter τ proposed by Addison et al.²⁵ is used here to describe the coordination geometry of a penta-coordinated metal ion, which is defined as $\tau = (\beta - \alpha)/60$, where β and α are the two largest angles around the metal center. For a regular square-pyramidal geometry τ is equal to zero, while it becomes unity for a regular trigonal-bipyramidal geometry. The τ value in **3** is 0.25 for Mn1, indicating a distorted square-pyramidal environment, while Mn2 is an almost ideal square-pyramidal geometry because of $\tau = 0.07$ for Mn2. The two adjacent Mn1 and Mn2 atoms are connected by three carboxyl groups to form a trigonal-bipyramidal binuclear unit $\text{Mn}_2(\text{OOC})_3$. The ligand *L*, on the other hand, is completely deprotonated and acts as an octadentate ligand. Similar to that of **1**,

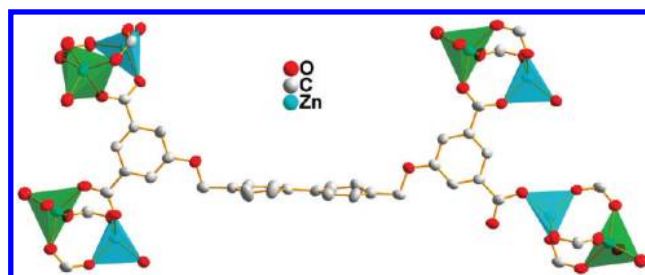


Figure 4. Building units of **2** (ellipsoids drawn at the 50% probability).

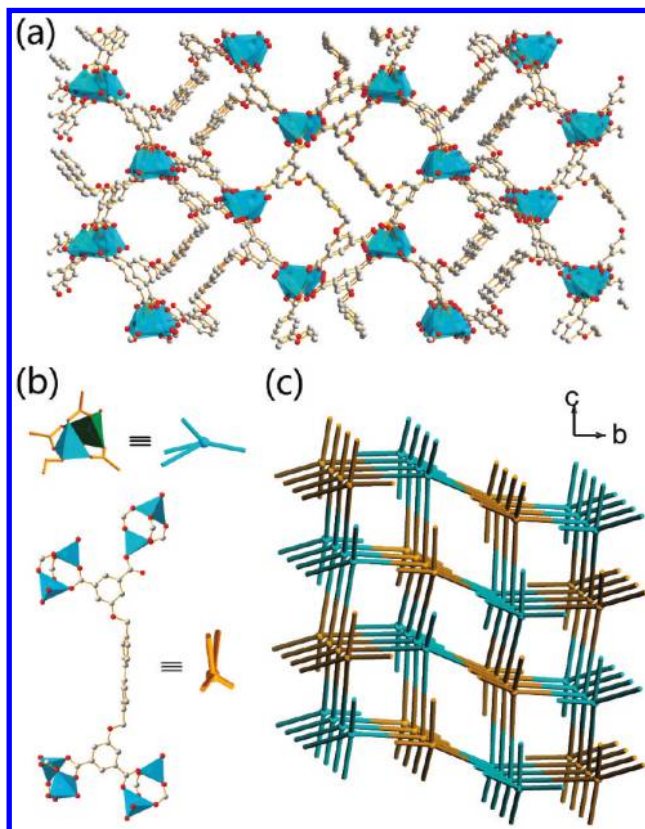


Figure 5. (a) Perspective view of crystalline framework, and topological representations of (b) SBUs, and (c) 3D framework of **2**.

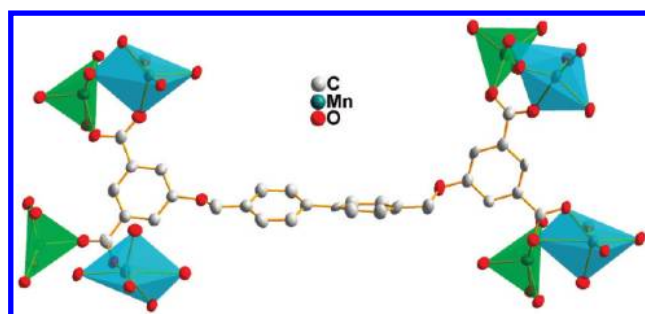


Figure 6. Building units of **3** (ellipsoids drawn at the 50% probability).

ligand *L* adopts bis-monodenate coordination modes and coordinates to eight Mn(II) ions. However, the *L* ligand in **3** is not in a planar coordination geometry as in **1** but shows obvious deviation with the

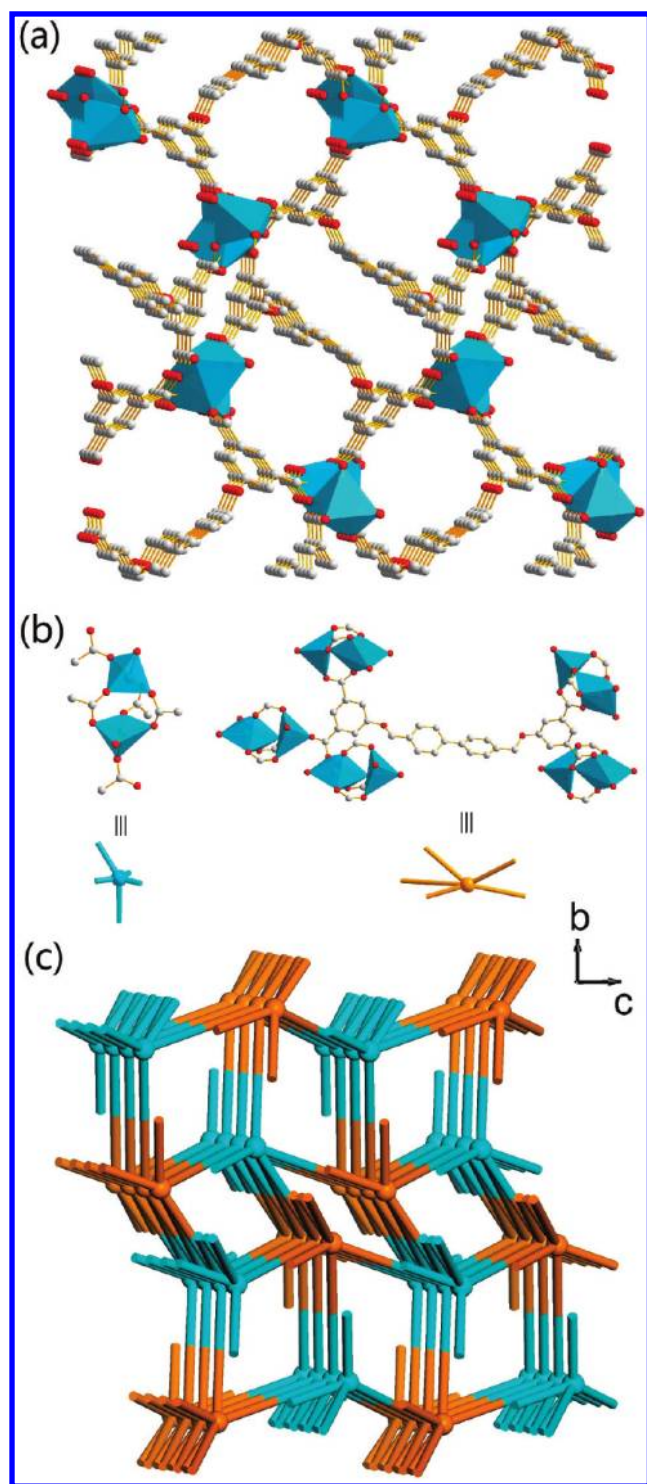


Figure 7. (a) Perspective view of the crystalline framework and topological representations of (b) SBUs, and (c) 3D framework of **3**.

dihedral angle of 27.4° between the two side phenyl rings bearing the carboxyl groups. In fact, no two of the four phenyl rings of the L ligand in **3** are in a plane. The biphenyl rings tilt away from each other with a dihedral angle of $26.6(1)^\circ$ and intersect the two side phenyl rings with the dihedral angles of $42.1(1)^\circ$ and $84.4(1)^\circ$, respectively.

The framework of **3** is built from binuclear $\text{Mn}_2(\text{OOC})_3$ units and octadentate L ligands (Figure 7). Each binuclear $\text{Mn}_2(\text{OOC})_3$ unit

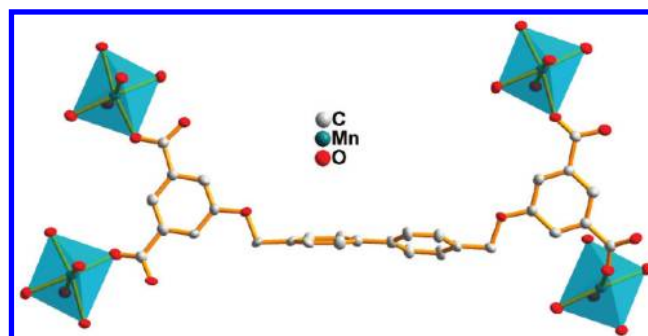


Figure 8. Building units of **4** (ellipsoids drawn at the 50% probability).

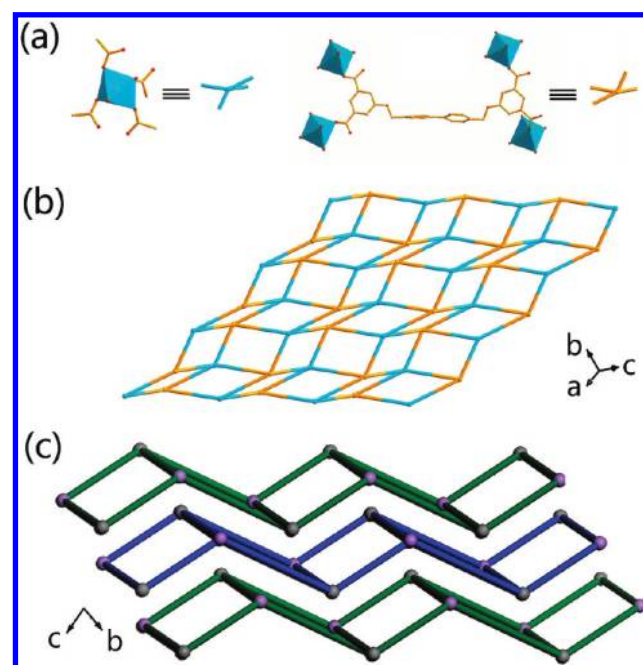


Figure 9. Topological representations of (a) SBUs, (b) a single layer, and (c) 3D packing of **4**.

adopts a trigonal-bipyramidal geometry, connecting to five carboxyl groups from five L ligands, while each L ligand links to five $\text{Mn}_2(\text{OOC})_3$ units. Considering both the binuclear $\text{Mn}_2(\text{OOC})_3$ unit and the L ligand as trigonal-bipyramidal nodes, the framework of **3** can thus be reduced to a binodal 5,5-connected net with a point (Schläfli) symbol of $4^3.6^6.8^4$.²⁴ From another point of view, the framework of **3** can be constructed from rod-shaped SBUs (Figure 7a). The SBUs are made of 2_1 helices, consisting of double 1D $\text{Mn}-\text{O}-\text{C}$ chains bridged by *m*-phenyl dicarboxylate groups. Each $\text{Mn}-\text{O}-\text{C}$ chain is composed of the binuclear units $\text{Mn}_2(\text{OOC})_3$ that are linked by bridging carboxyl groups from the axial positions to form an infinite 1D chain in the *a* crystallographic direction. The SBU rods run parallel the *a* direction and are connected to six neighboring ones by L ligands, resulting in parallel rod packing of hex type²² with two kinds of rectangle channels of 6.92×10.46 and $3.35 \times 16.56 \text{ \AA}^2$ in size, respectively. Inside the channels reside the guest water molecules, which form weak van der Waals interactions with the host framework. The total voids are estimated to be 106.0 \AA^3 per unit cell, comprising only 3.1% of the total crystal volume.

[Mn(H₂L)(DMA)(H₂O)] · (DMA)(H₂O) (4**).** Compound **4** crystallizes in the triclinic space group $P\bar{1}$. The asymmetric unit

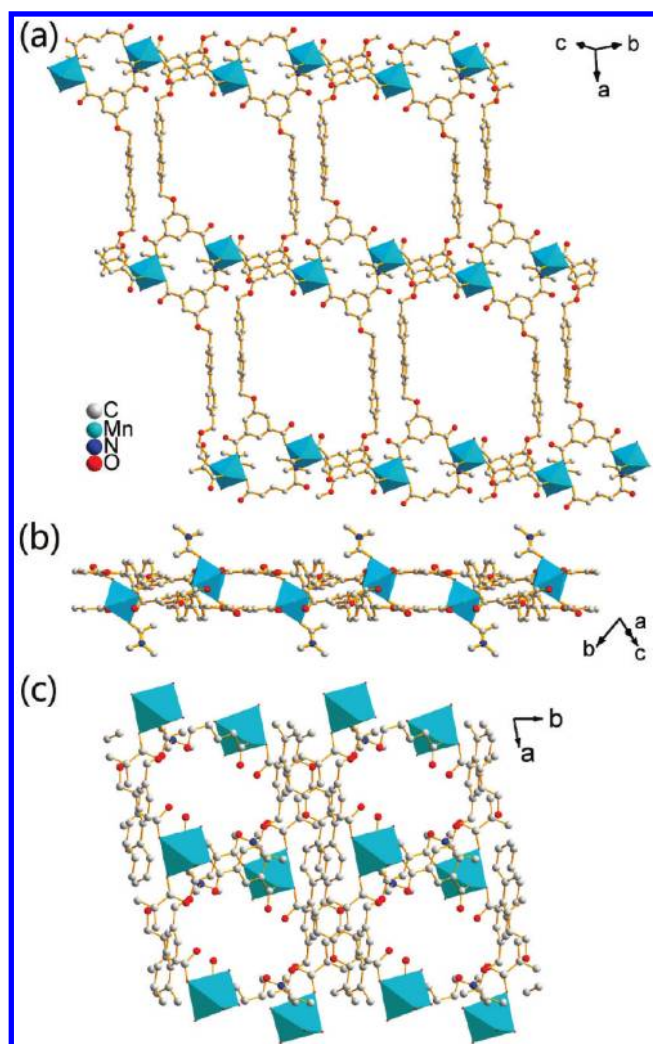


Figure 10. (a) Front and (b) side views of a single layer, and (c) 3D packing of **4**. The guest molecules are omitted for clarity.

consists of each of Mn^{2+} cation, L ligand, coordinate DMA and water, and guest DMA and water molecules. As shown in Figure 8, the Mn1 atom is octahedrally coordinated by one O atom of DMA molecule, one oxygen atom of one water molecule, and four oxygen atoms from four different L ligands. All the Mn–O bond lengths are in agreement with those generally found in the literature.^{23c} The ligand L is half deprotonated as in an H_2L^{2-} form and acts as a quadridentate ligand. The geometry of the L ligand in **4** resembles that in compound **3**. The dihedral angle between the two side phenyl rings bearing the carboxyl groups is ca. 22.90° , while those between the two middle biphenyl, and the two side-middle phenyl rings are $23.9(1)$, $65.5(1)$, and $75.9(1)$, respectively.

Compound **4** possesses a 2D structure made of 4-connecting mononuclear Mn atoms and half-deprotonated L ligands (Figure 9 and 10). Each half-deprotonated L ligand adopts monodentate coordination modes, connecting to four Mn cations in a nearly planar geometry, while each Mn atom is linked to four L ligands. This arrangement gives rise to a (4,4)-connecting 2D sql/Shubnikov topologic grid sheet with large elliptical rings of $18.7 \times 6.3 \text{ \AA}$ in diagonal distances. The 2D sheet are stacked over each other in an ABAB fashion along the $[111]$ direction to form

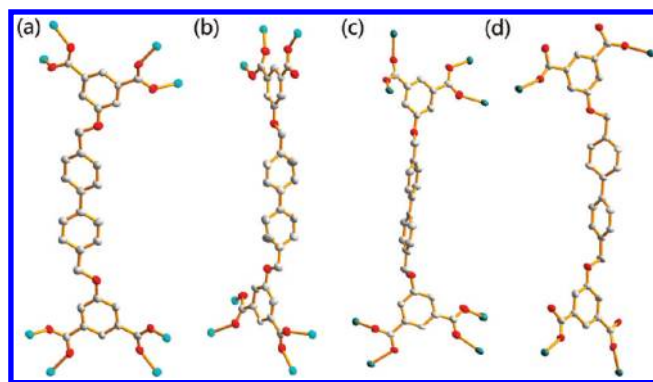


Figure 11. Coordination modes of L in (a) **1**, (b) **2**, (c) **3**, and (d) **4**.

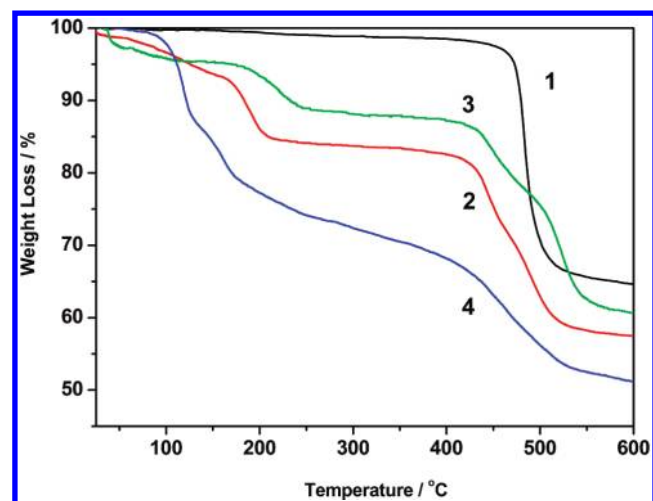


Figure 12. TG curves of **1–4**.

a 3D van der Waals network. The coordinate DMA molecules on Mn atoms on one sheet protrude into the cavities of the neighboring sheets. The one-dimensional elliptical channels measuring $9.6 \times 6.3 \text{ \AA}^2$ in diagonal distances run along the c axis, inside which guest DMA and water molecules reside. These guest molecules are involved in the host–guest hydrogen-bonding interactions (e.g., $\text{O1W} \cdots \text{H1WA} \cdots \text{O12}$, $\text{O9} \cdots \text{H9C} \cdots \text{O2W}$, and $\text{C24} \cdots \text{H24} \cdots \text{O12}$, see Table S2, Supporting Information). The total voids are estimated to be 360.1 \AA^3 per unit cell, comprising 19.1% of the total crystal volume.

Ligand Conformation and the Role of the Solvent. Owing to its flexibility, the ligand L exhibits diverse coordination modes in compounds **1–4** (Figure 11). Its four carboxylate groups can fully deprotonated as in **1**, **2**, and **3** or partially deprotonated as in **4**, coordinating to eight metal ions in **1** and **3**, seven metal ions in **2** and four metal ions in **4** in a bis-monodentate and/or a monodentate mode, respectively. Furthermore, the side phenyl rings bearing two carboxylate groups in L can twist around the middle biphenyl rings to meet different coordination environments. The side phenyl rings tilt away from the connecting biphenyl rings with dihedral angles of $10.3(2)$, $79.2(1)$ – $86.4(1)$, $42.1(1)$ – $84.4(1)$, and $65.5(1)$ – $75.9(1)^\circ$ in **1**, **2**, **3**, and **4**, respectively. As a result, the dihedral angles between the two side phenyl rings in **1–4** are $4.5(2)$, $11.4(1)$, $27.4(1)$, and $22.9(1)^\circ$, respectively. In other words, the L ligand in **1** and **2** is in a nearly planar coordination geometry, while it is in a

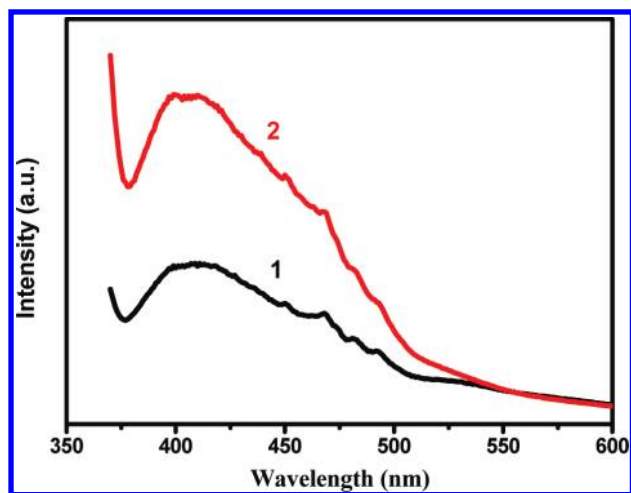


Figure 13. Photoluminescent spectra of 1 and 2 in the solid state at room temperature.

distorted tetrahedral coordination geometry in 3 and 4. These lead to the formation of four different structures in 1–4.

The varieties of coordination modes of L in 1–4 resemble its analogue ligands L8¹² and L9¹³ (Scheme 1). Ligands L8 and L9 have been shown to exhibit different coordination geometries in a bis-monodentate mode linking to eight to six metal ions in a fully deprotonated form or to two metal ions in a half-deprotonated one. The aryloxy groups in L8 and L9 can twist away from the plane of the central benzene ring or around the central CH₂ unit at the requirements of the coordination environments, leading to various new MOFs. However, the coordination chemistry of ligands L is different with that of rigid ligands L5,⁸ L6,^{9,10} and L7,^{10,11} although they all are tetracarboxylate ligands, each bearing two isophthalic acids. These ligands adopt planar coordination geometries in almost all cases. These rigid ligands have been often chosen in constructions of coordination polymers with specific structures (e.g., NbO type) since they allow for a certain control of the steric consequences in the assembly process. However, flexible ligands have their own merits because they can expand, shrink, or distort their soft coordination geometries, as exemplified by L, resulting in new coordination polymers with intriguing structural topology.

It is probably because of the flexibility of ligand L that the formation of coordination polymers 1–4 are strongly dependent on the synthetic conditions such as the solvent. The Zn complexes 1 and 2 were synthesized from CH₃CN–H₂O and DMF–H₂O solvent systems under otherwise the same conditions, respectively. However, 1 ([Zn₂(L)]·CH₃CN) is a 3D pcu rod-packing framework with guest molecules CH₃CN, while 2 ([Zn₄(L)₂(H₂O)₄]·5H₂O) possesses a doubly interpenetrated sra net incorporated with coordination and guest water molecules. These suggest that CH₃CN interacts more strongly than water with the framework of 1, while water has more affinity to Zn than DMF in 2. The Mn complexes 3 and 4 were also formed under similar conditions by using different solvents DMF–H₂O and DMA–H₂O. However, both DMA and water are more apt to coordinate with Mn than with DMF, resulting in a binodal (5,5)-connected 4³.6⁶.8 net with coordination and guest water in 3 ([Mn₂(L)(H₂O)₂]·2H₂O) but a (4,4)-connecting 2D sql sheet with both coordination and guest DMA and water molecules in 4 ([Mn(H₂L)(DMA)(H₂O)]·DMA·H₂O). In four

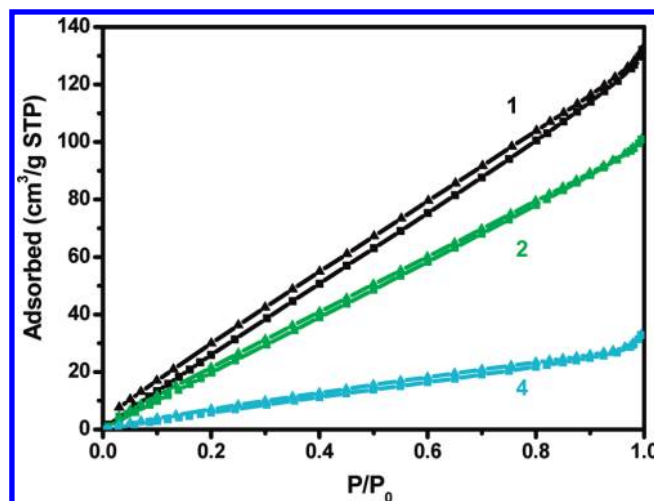


Figure 14. Nitrogen adsorption–desorption isotherms of 1, 2, and 4 at 77 K.

complexes, the solvent molecules either coordinate with the metal ions, or form hydrogen bonds or van der Waals interactions with the framework to stabilize the structure. Apparently, these solvent molecules with different sizes, polarities, and coordination abilities present in the coordination spheres of the metal ions exert their influence on the formation of coordination polymers. These in combination with the flexibility of the ligand result in different complexes with intriguing structure topologies. The DMF molecules, though not present in the final products, may still contribute to the formation of 2 and 3 by regulating the pH values and/or serving as structure directing agents.²⁶

Thermal Analysis. To estimate the stability of complexes 1–4, the TG analyses were carried out, as shown in Figure 12. For complex 1, the weight loss of 2.5% from RT to 450 °C corresponds to partial departure of acetonitrile guests (calcd 5.7%). The structure subsequently collapsed with an abrupt weight loss of 32.3% as a result of ligand decomposition (calcd 29.9% for OCH₂PhPhCH₂O). Complex 2 lost surface water from RT to ca. 100 °C (ca. 3.8%) and three guest water molecules (observed 3.3%, calcd 3.6%) from ca. 100 to ca. 160 °C. The coordinate water molecules and two guest water molecules were lost from ca. 160 to ca. 205 °C (observed 7.9%, calcd 7.2%). The framework began to decompose at ca. 400 °C (observed 24.3%, calcd 24.3% for CH₂PhPhCH₂). For complex 3, the weight loss of 2.6% below ca. 50 °C is likely due to the loss of surface water. The loss of guest and coordinate water molecules occurred from ca. 65 to ca. 300 °C (observed 9.2%, calcd 10.0%). The framework collapsed from ca. 410 °C with losses of parts of ligands (observed 26.0%, calcd 25.3% for CH₂PhPhCH₂). For complex 4, the weight loss of 12.7% from RT to ca. 130 °C corresponds to the loss of guest water and DMA molecules (calcd 13.0%). The loss of coordinate water and DMA molecules started from ca. 150 to ca. 250 °C (observed 13.2%, calcd 13.0%). The further weight loss is due to the decomposition of the ligands (observed 21.9%, calcd 22.6% for CH₂PhPhCH₂).

Photoluminescence of 1 and 2. Considering that d¹⁰ metal complexes usually exhibit excellent luminescent properties, the photoluminescent properties of 1 and 2 were investigated. As shown in Figure 13, both complexes 1 and 2 exhibit similar photoluminescence with λ_{max} = 420 nm upon excitation at 350 nm, while the free L ligand shows no obvious emissions.

The emissions of **1** and **2** are probably due to the chelation of the ligand to the metal center, which may result in $\pi_L \rightarrow \pi_L^*$ ligand-to-metal charge transfer (LMCT).²⁷ The coordination enhances the “rigidity” of the ligand and thus reduces the loss of energy through a radiationless pathway, which facilitates the $\pi_L \rightarrow \pi_L^*$ transitions. The difference in photoluminescence spectra of **1** and **2** may be attributed to the different coordination environments of the Zn(II) and crystal packing in the solid state.

Gas Adsorption Properties. X-ray crystal structure and thermal studies show that complexes **1–4** possess the microporous structure with removable guest molecules in open channels. These complexes may serve as potential gas adsorption/separation materials. To investigate their porosity, the nitrogen adsorption measurements at 77 K were performed. Prior to the measurements, all the samples were activated by using the procedure described by Zhou.²⁸ As depicted in Figure 14, complexes **1**, **2**, and **4** showed permanent porosity, while **3** exhibited no measurable adsorption for N₂ gas. It is not surprising because of the lack of free solvent accessible voids in **3** as calculated by PLATON.²¹ All the N₂ adsorption isotherms of **1**, **2** and **4** are of type III, indicating the weak interactions between nitrogen molecules and the host frameworks. The hystereses between adsorption and desorption isotherms of **1**, **2** and **4** are probably due to the retaining of N₂ in the flexible small channels as a result of pore opening comparable to the size of N₂ molecule. The Brunauer–Emmett–Teller (BET) surface areas are calculated from N₂ adsorption isotherms to be 216, 117, and 53 m²/g, respectively.

CONCLUSIONS

Four new metal–organic coordination polymers of Zn(II) and Mn(II) were solvothermally synthesized by using a quadricarboxylate ligand. The formation of the four complexes is strongly dependent on the solvent and metals used during the synthesis. The four complexes possess interesting topological structures, three of which have permanent porosity. The ligand in these complexes exhibits rich coordination chemistry owing to its semirigid flexibility. This study shows that using semirigid multidentate ligands in combination of control of synthetic parameters such as solvents and metals could lead to new compounds with interesting structures and properties.

ASSOCIATED CONTENT

Supporting Information. Crystallographic information (cif) files, XRPD, and tables for interatomic distances and angles. This material is available free of charge via the Internet at <http://pubs.acs.org>.

AUTHOR INFORMATION

Corresponding Author

*E-mail: hbdu@nju.edu.cn.

ACKNOWLEDGMENT

We are grateful for financial support from the National Basic Research Program (2011CB808704 and 2007CB925101) and the National Natural Science Foundation of China (21021062 and 20931004).

REFERENCES

- (1) (a) Farha, O. K.; Malliakas, C. D.; Kanatzidis, M. G.; Hupp, J. T. *J. Am. Chem. Soc.* **2009**, *132*, 950. (b) Kitagawa, S.; Kitaura, R.; Noro, S. *Angew. Chem., Int. Ed.* **2004**, *43*, 2334. (c) Li, J. R.; Kuppler, R. J.; Zhou, H. C. *Chem. Soc. Rev.* **2009**, *38*, 1477. (d) Ma, S.; Zhou, H. C. *Chem. Commun.* **2009**, *46*, 44. (e) Rosi, N. L.; Eckert, J.; Eddaoudi, M.; Vodak, D. T.; Kim, J.; O’Keeffe, M.; Yaghi, O. M. *Science* **2003**, *300*, 1127. (f) Yaghi, O. M.; O’Keeffe, M.; Ockwig, N. W.; Chae, H. K.; Eddaoudi, M.; Kim, J. *Nature* **2003**, *423*, 705. (g) Zhang, J. P.; Chen, X. M. *J. Am. Chem. Soc.* **2009**, *131*, 5516. (h) Chen, B.; Xiang, S.; Qian, G. *Acc. Chem. Res.* **2010**, *43*, 1115.
- (2) (a) Chen, X. D.; Wu, H. F.; Zhao, X. H.; Zhao, X. J.; Du, M. *Cryst. Growth Des.* **2006**, *7*, 124. (b) Liu, J. Q.; Wang, Y. Y.; Zhang, Y. N.; Liu, P.; Shi, Q. Z.; Batten, S. R. *Eur. J. Inorg. Chem.* **2009**, *2009*, 147. (c) Withersby, M. A.; Blake, A. J.; Champness, N. R.; Cooke, P. A.; Hubberstey, P.; Li, W. S.; Schroder, M. *Inorg. Chem.* **1999**, *38*, 2259. (d) Hirotsu, M.; Kuwamura, N.; Kinoshita, I.; Kojima, M.; Yoshikawa, Y.; Ueno, K. *Dalton Trans.* **2009**, 7678. (e) Du, J. L.; Hu, T. L.; Li, J. R.; Zhang, S. M.; Bu, X. H. *Eur. J. Inorg. Chem.* **2008**, *2008*, 1059. (f) Fang, R. Q.; Zhang, X. M. *Inorg. Chem.* **2006**, *45*, 4801. (g) Cui, F. Y.; Huang, K. L.; Xu, Y. Q.; Han, Z. G.; Liu, X.; Chi, Y. N.; Hu, C. W. *CrystEngComm* **2009**, *11*, 2757.
- (3) (a) Eddaoudi, M.; Moler, D. B.; Li, H.; Chen, B.; Reineke, T. M.; O’Keeffe, M.; Yaghi, O. M. *Acc. Chem. Res.* **2001**, *34*, 319. (b) Perry, J. J., IV; Perman, J. A.; Zaworotko, M. J. *Chem. Soc. Rev.* **2009**, *38*, 1400.
- (4) Zang, S.; Su, Y.; Li, Y.; Ni, Z.; Meng, Q. *Inorg. Chem.* **2005**, *45*, 174.
- (5) (a) Sun, L. X.; Qi, Y.; Wang, Y. M.; Che, Y. X.; Zheng, J. M. *CrystEngComm* **2010**, *12*, 1540. (b) Wang, X. L.; Qin, C.; Wang, E. B.; Xu, L. *Eur. J. Inorg. Chem.* **2005**, *2005*, 3418.
- (6) (a) Zang, S.; Su, Y.; Li, Y. Z.; Lin, J.; Duan, X.; Meng, Q.; Gao, S. *CrystEngComm* **2009**, *11*, 122. (b) Zang, S.; Su, Y.; Duan, C.; Li, Y.; Zhou, H.; Meng, Q. *Chem. Commun.* **2006**, *48*, 4997.
- (7) (a) Su, Y.; Zang, S.; Li, Y.; Zhou, H.; Meng, Q.; Gao, S. *Cryst. Growth Des.* **2007**, *7*, 1277. (b) Zang, S.; Su, Y.; Song, Y.; Li, Y.; Ni, Z.; Zhou, H.; Meng, Q. *Cryst. Growth Des.* **2006**, *6*, 2369.
- (8) Cairns, A. J.; Perman, J. A.; Wojtas, L.; Kravtsov, V. C.; Alkordi, M. H.; Eddaoudi, M.; Zaworotko, M. J. *J. Am. Chem. Soc.* **2008**, *130*, 1560.
- (9) (a) Chen, B.; Ockwig, N. W.; Millward, A. R.; Contreras, D. S.; Yaghi, O. M. *Angew. Chem., Int. Ed.* **2005**, *44*, 4745. (b) Chen, B.; Ockwig, N. W.; Fronczek, F. R.; Contreras, D. S.; Yaghi, O. M. *Inorg. Chem.* **2005**, *44*, 181.
- (10) (a) Lin, X.; Jia, J.; Zhao, X.; Thomas, K. M.; Blake, A. J.; Walker, G. S.; Champness, N. R.; Hubberstey, P.; Schröder, M. *Angew. Chem., Int. Ed.* **2006**, *45*, 7358. (b) Lin, X.; Telepeni, I.; Blake, A. J.; Dailly, A.; Brown, C. M.; Simmons, J. M.; Zoppi, M.; Walker, G. S.; Thomas, K. M.; Mays, T. J.; Hubberstey, P.; Champness, N. R.; Schröder, M. *J. Am. Chem. Soc.* **2009**, *131*, 2159.
- (11) (a) Yang, S.; Lin, X.; Blake, A. J.; Walker, G. S.; Hubberstey, P.; Champness, N. R.; Schröder, M. *Nat. Chem.* **2009**, *1*, 487. (b) Yang, S.; Lin, X.; Dailly, A.; Blake, A. J.; Hubberstey, P.; Champness, N. R.; Schröder, M. *Chem.—Eur. J.* **2009**, *15*, 4829.
- (12) Qiu, W.; Perman, J. A.; Wojtas, L.; Eddaoudi, M.; Zaworotko, M. J. *Chem. Commun.* **2010**, *46*, 8734.
- (13) Pan, Z.; Zheng, H.; Wang, T.; Song, Y.; Li, Y.; Guo, Z.; Batten, S. R. *Inorg. Chem.* **2008**, *47*, 9528.
- (14) (a) Ren, S. B.; Zhou, L.; Zhang, J.; Zhu, Y. L.; Du, H. B.; You, X. Z. *CrystEngComm* **2010**, *12*, 1635. (b) Ren, S. B.; Zhou, L.; Zhang, J.; Du, H. B.; You, X. Z. *CrystEngComm* **2009**, *11*, 1834. (c) Liang, L. L.; Ren, S. B.; Zhang, J.; Li, Y. Z.; Du, H. B.; You, X. Z. *Cryst. Growth Des.* **2010**, *10*, 1307. (d) Zhang, J.; Xue, Y. S.; Liang, L. L.; Ren, S. B.; Li, Y. Z.; Du, H. B.; You, X. Z. *Inorg. Chem.* **2010**, *49*, 7685.
- (15) (a) Liang, L. L.; Ren, S. B.; Wang, J.; Zhang, J.; Li, Y. Z.; Du, H. B.; You, X. Z. *CrystEngComm* **2010**, *12*, 2669. (b) Liang, L. L.; Zhang, J.; Ren, S. B.; Ge, G. W.; Li, Y. Z.; Du, H. B.; You, X. Z. *CrystEngComm* **2010**, *12*, 2008. (c) Liang, L. L.; Ren, S. B.; Zhang, J.; Li, Y. Z.; Du, H. B.; You, X. Z. *Dalton Trans.* **2010**, *39*, 7723.

- (16) Zhang, Q.; Bu, X.; Lin, Z.; Wu, T.; Feng, P. *Inorg. Chem.* **2008**, *47*, 9724.
- (17) Pan, Y.; Ford, W. T. *J. Org. Chem.* **1999**, *64*, 8588.
- (18) SMART, and SADABS; Bruker AXS Inc.: Madison, Wisconsin, USA.
- (19) Sheldrick, G. M. *Acta Crystallogr.* **2008**, *A64*, 112.
- (20) (a) Tynan, E.; Jensen, P.; Kruger, P. E.; Lees, A. C. *Chem. Commun.* **2004**, 776. (b) Nättinen, K. I.; Rissanen, K. *Inorg. Chem.* **2003**, *42*, 5126. (c) Du, M.; Wang, X. G.; Zhang, Z. H.; Tang, L. F.; Zhao, X. J. *CrystEngComm* **2006**, *8*, 788.
- (21) Spek, A. L. *J. Appl. Crystallogr.* **2003**, *36*, 7.
- (22) Rosi, N. L.; Kim, J.; Eddaoudi, M.; Chen, B.; O'Keeffe, M.; Yaghi, O. M. *J. Am. Chem. Soc.* **2005**, *127*, 1504.
- (23) (a) Zevaco, T. A.; Görls, H.; Dinjus, E. *Polyhedron* **1998**, *17*, 2199. (b) Wang, G. L.; Yang, X. L.; Liu, Y.; Li, Y. Z.; Du, H. B.; You, X. Z. *Inorg. Chem. Commun.* **2008**, *11*, 814. (c) Orpen, A. G.; Brammer, L.; Allen, F. H.; Kennard, O.; Watson, D. G.; Taylor, R. *Dalton Trans.* **1989**, No. Suppl., S1.
- (24) (a) O'Keeffe, M.; Eddaoudi, M.; Li, H.; Reineke, T.; Yaghi, O. M. *J. Solid State Chem.* **2000**, *152*, 3. (b) Blatov, V. A. *IUCr CompComm Newsl.* **2006**, *4*. (c) Blatov, V. A.; Carlucci, L.; Ciani, G.; Proserpio, D. M. *CrystEngComm* **2004**, *6*, 378. (d) Blatov, V. A.; O'Keeffe, M.; Proserpio, D. M. *CrystEngComm* **2010**, *12*, 44.
- (25) Addison, A. W.; Rao, T. N.; Reedijk, J.; Rijn, J.; Verschoor, G. C. *Dalton Trans.* **1984**, 1349.
- (26) (a) Ghosh, S. K.; Kitagawa, S. *CrystEngComm* **2008**, *10*, 1739. (b) Tynan, E.; Jensen, P.; Kruger, P. E.; Lees, A. C. *Chem. Commun.* **2004**, 776.
- (27) (a) Zheng, S. L.; Yang, J. H.; Yu, X. L.; Chen, X. M.; Wong, W. T. *Inorg. Chem.* **2003**, *43*, 830. (b) Zheng, S. L.; Tong, M. L.; Tan, S. D.; Wang, Y.; Shi, J. X.; Tong, Y. X.; Lee, H. K.; Chen, X. M. *Organometallics* **2001**, *20*, 5319.
- (28) Ma, S.; Simmons, J. M.; Sun, D.; Yuan, D.; Zhou, H. C. *Inorg. Chem.* **2009**, *48*, 5263.